Mem. S.A.It. Vol. 75, 682

Memorie della

Rotating models of low metallicity AGB stars with STAREVOL

T. Decressin[1], C. Charbonnel[1,2], L. Siess[3] & A. Palacios[3]

[1] Geneva Observatory, 51 ch des Maillettes, 1290 Sauverny, Switzerland
e-mail: Thibaut.Decressin@obs.unige.ch
[2] LA2T, OMP, CNRS UMR 5572, 14 Av. E. Belin, 31400 Toulouse, France
[3] Institut d'Astronomie et d'Astrophysique, ULB, CP 226 bd du Triomphe, B-1050 Brussels, Belgium

Abstract. We present rotating models of a 7 $M_\odot$ star at $Z = 10^{-5}$ and analyze how rotational mixing affects their evolution, nucleosynthesis and yields. We confirm that rotational mixing enables a large production of primary ^{14}N and show that it is responsible for a steep increase in the mass loss rate during the early-AGB phase. We also address the origin of the O-Na anti-correlation in globular clusters. We show that rotating models experience a large surface O-enhancement during second dredge-up which indicates that massive rotating AGB stars are not responsible for this anti-correlation in the so-called pollution scenario.

Key words. AGB stars – rotation

1. STAREVOL

We use the stellar evolution code STAREVOL to compute the models presented in this paper. This code was originally developed by *Manuel Forestini* (Forestini et al. 1991). It allows the computation of stars in the mass range 0.1 to 60 $M_\odot$, from the pre-main sequence (with possible accretion) up to Ne burning. It includes different transport processes for angular momentum and chemicals.

The main physical inputs are the following (see Siess et al. 1997, 2000 for more details) : the opacity tables come from OPAL (Iglesias & Rogers 1996) for $T > 8000$ K, and from Alexander & Ferguson (1994) at lower temperatures. We follow the evolution of 53 chemical species from ^{1}H to ^{37}Cl and use the nuclear reaction rates from NACRE (Angulo et al. 1999) and when not available from Caughlan & Fowler (1988). To describe convection we use the MLT formalism with $\alpha_{\rm MLT} = 1.75$. For the treatment of mass loss, we use Reimers' (1975) formula with $\eta_{\rm R} = 0.5$ up to the end of core He burning and then switch to Blöcker's (1995) law on the AGB with $\eta_{\rm B} = 0.05$. In all cases, the mass loss is scaled with metallicity by a factor of $\sqrt{Z/Z_\odot}$. In some models we include overshooting below the convective envelope (hereafter OV) following Herwig's (2000) prescription with $f_{\rm over} = 0.016$. This extra mixing is needed to trigger third dredge-ups in our models (hereafter 3DUP).

We follow Zahn's (1992) and Maeder & Zahn's (1998) formalism for rotational trans-

Send offprint requests to: T. Decressin
Correspondence to: Geneva Observatory, 51 ch des Maillettes, 1290 Sauverny

port of angular momentum and chemicals. We refer to Palacios et al. (2003) for physical and numerical details. The effects of both meridional circulation (MC) and shear turbulence are taken into account.

The following equation is used to compute the transport of angular momentum:

$$\overbrace{\rho \frac{d}{dt}\left[r^2\Omega\right]}^{\text{contraction or expansion}} = \overbrace{\frac{1}{5r^2}\frac{\partial}{\partial r}\left[\rho r^4 \Omega U\right]}^{\text{advection by MC}} + \underbrace{\frac{1}{r^2}\frac{\partial}{\partial r}\left[\rho \nu_{\rm v} r^4 \frac{\partial \Omega}{\partial r}\right]}_{\text{diffusion by shear}}, \quad (1)$$

where U is the vertical component of the meridional circulation and $\nu_{\rm v}$ is the vertical viscosity. The meridional circulation advects angular momentum and the shear acts as a diffusive process. This formalism has been extensively used by the Geneva group (see Meynet & Maeder 2002 for example) in their works on rotating massive stars and in low mass stars by Palacios et al. (2003, 2005) both on the main sequence and on the RGB. Note that this treatment differs from that of Langer et al. (1999) who do not include the advective term in Equation 1.

The transport of chemical species is computed with the following equation:

$$\rho \frac{dc_i}{dt} = \frac{1}{r^2}\frac{\partial}{\partial r}\left[r^2 \rho (D_{\rm eff} + D_{\rm v}) \frac{\partial c_i}{\partial r}\right], \quad (2)$$

where $D_{\rm eff}$ and $D_{\rm v}$ represent the diffusion coefficients associated with meridional circulation and vertical turbulence, respectively. The concentration of element i is denoted by c_i. In the star we consider here, atomic diffusion is never significant and not accounted for.

Rotation also affects mass loss and we follow Maeder & Meynet's (2001) prescription :

$$\frac{\dot{M}(\Omega)}{\dot{M}(0)} = \frac{(1-\Gamma)^{1/\alpha - 1}}{[1 - \frac{\Omega^2}{2\pi G \rho_m} - \Gamma]^{1/\alpha - 1}}, \quad (3)$$

where Γ is the Eddington factor for electron scattering opacities, α is an empirical force multiplier varying from 0.52 to 0.15 with the effective temperature and $\frac{\Omega^2}{2\pi G \rho_m}$ is the ratio of the rotational velocity to the break-up velocity. From Equation 3, mass loss increases in rotating stars due to the lower effective gravity but this effect remains very weak in our models. Finally, let us note that we do not take into account the effects of centrifugal forces on the stellar structure equations.

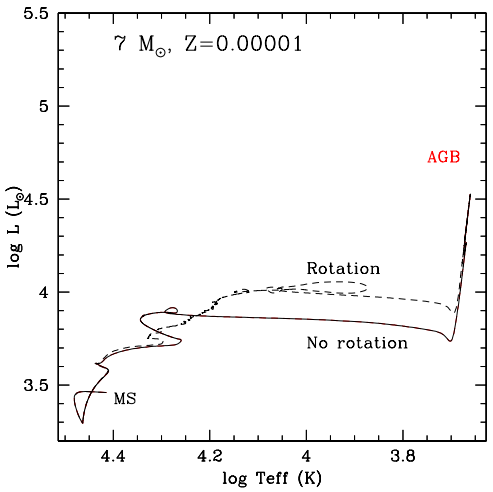

Fig. 1. HR diagram for the models of 7 $M_\odot$ star at $Z = 10^{-5}$ in the standard case (solid line) and with rotation (dashed line)

In this study, we present four different models of a 7 $M_\odot$ star at $Z = 10^{-5}$. Case (A) is the standard non-rotating model including OV during the AGB phase. Cases (B-D) include rotational mixing from the ZAMS up to the end of central He-burning with an initial velocity of 300 km/s. Then during the AGB phase, we stop the transport of angular momentum as described in Equation 1 and consider different options. In case (B), the rotational profile is derived from local angular momentum conservation and used to compute the diffusion coefficients entering the equation for chemicals transport (Equation 2). In case (C), we do not treat rotational mixing anymore but instead include OV below the convective envelope, as in case (A) and in case (D), we stop all kind of extra mixing.

Table 1. Lifetimes on pre-AGB phases, core mass at the end of central He-burning and depth of the envelope during the 2DUP for models of a 7 $M_\odot$ stars at $Z = 10^{-5}$.

	standard case A	rotation cases BCD
$\tau_{\rm MS}$ (10^7 yr)	3.74	3.76
$\tau_{\rm HeB}$ (10^6 yr)	6.28	10.17
$\tau_{\rm pre\text{-}AGB}$ (10^7 yr)	4.49	4.93
$M_{\rm CO}(M_\odot)$	0.80	0.86
$M_{\rm 2DUP}$ ($M_\odot$)	1.00	1.02 (B) 1.09 (CD)

2. Main results

2.1. Evolutionary features

Figure 1 illustrates the effects of rotation in the HR diagram. In the high mass and low metallicity models we consider, there is no RGB phase nor first dredge-up. The rotating models are more luminous. This can be attributed to the opacity decrease in the envelope as a result of He diffusion.

Table 1 presents the lifetimes of different phases. Rotation does not significantly modify the main sequence duration. On the contrary, the phase of central He-burning is lengthened since diffusion brings fresh helium from the H-burning shell into the core. In the end, the pre-AGB phase is 10% longer in the rotating model than in the standard case. As a consequence of mixing, the rotating model starts the ascent of the TP-AGB with a CO core about 8% more massive than the standard model.

Figure 2 shows the effects of rotation on the chemical profiles at the end of central He-burning. In the standard model, nitrogen is produced outside the core in the H burning shell (HBS) from the carbon and oxygen originally present in the star and is therefore secondary. In the rotating model, diffusion spreads the chemical profiles smoothing the discontinuity at the edge of the core. In this case, carbon and oxygen diffuse from the core into the HBS where they are converted by the CNO cycle into nitrogen which this time is essentially primary. We also note the production of a small

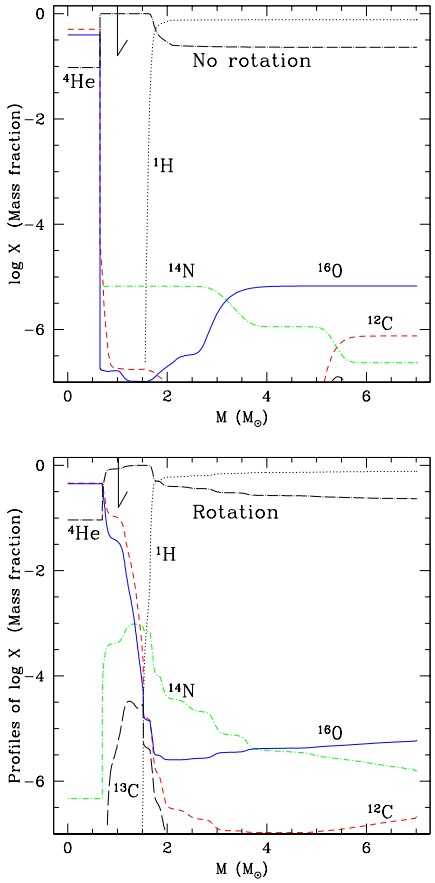

Fig. 2. Chemical profiles at the end of central He-burning for case A (top) and cases BCD (bottom). We show the profiles of protons (dotted lines), ^{4}He (long dashed-dotted lines),^{12}C (short dashed lines), ^{13}C (long dashed lines), ^{14}N (dotted-dashed lines) and ^{16}O (solid lines). The maximum extent of the convective envelope during the 2DUP is indicated by the arrow.

pocket of ^{13}C as a result of proton captures on ^{12}C.

The evolution of the surface abundances of selected isotopes is shown in Figure 3. Contrary to the standard case (A), in the rotating models ^{12}C and ^{14}N surface abundances are already modified during the main sequence and central He-burning. The subsequent sec-

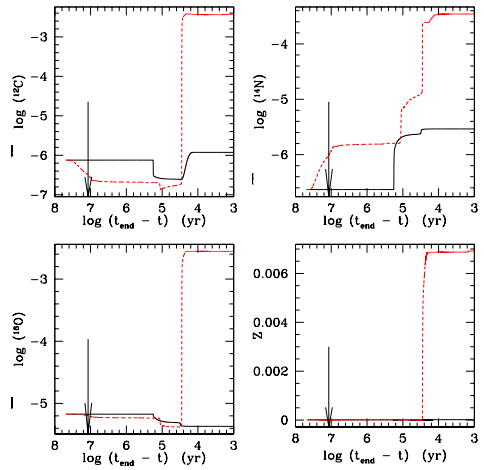

Fig. 3. Evolution of the surface chemical abundances for the model without rotation (solid lines) and the rotating model (D) (dashed lines) for ^{12}C, ^{14}N, ^{16}O, and the total metallicity. The arrow indicates the end of the MS. The time is counted from the last computed model.

ond dredge-up (2DUP, $\log(t_{\rm end} - t) \sim 4.4$ in Figure 3) is responsible for the major changes of the envelope chemical composition and the TP-AGB phase will barely affect this chemical imprint. In the rotating models the 2DUP is shallower than in the standard case but it produces a larger surface enrichment of ^{12}C, ^{14}N and ^{16}O. This can be easily understood from Figure 2 when comparing the internal chemical profiles at the arrow's location. Note that in case (B), the maintenance of rotational mixing in the interior is responsible for even larger surface modifications during the 2DUP compared to cases (C) and (D).

The rotating models also show a large increase in the overall metallicity during the 2DUP since the convective envelope brings matter which is partially processed in the He-burning core.

Between the end of the 2DUP and the occurrence of the first thermal pulse, the rotating models lose about 5 $M_{\odot}$ (Table 2), which represents around 80% of the total amount of mass they will eject. In comparison the standard case experiences almost no mass loss at this stage. This phenomenon results from the strong dependence of the adopted mass loss rate on the luminosity which is much higher in the rotating models.

Table 2 presents the main characteristics of the TP-AGB phase. We simply report the early development of 3DUP in models including overshooting (A and C) and the presence of hot bottom burning in all the models.

Table 2. Main features of the TP-AGB phase : presence of 3DUP (starting at pulse number i), efficiency of 3DUP, presence of HBB declared when the temperature at the bottom of the convective envelope exceeds 40×10^6K, total stellar mass at the beginning of TP-AGB and at the end of the computation. For case B, the model is still on the early-AGB phase (work in progress).

	3DUP	$\lambda_{\rm max}$	HBB	$M_{\rm TP}$ ($M_{\odot}$)	$M_{\rm end}$ ($M_{\odot}$)
A	Yes (7)	0.75	Yes	6.98	1.50
B					2.00
C	Yes (8)	0.25	Yes	2.62	1.49
D	No	–	Yes	2.70	1.35

2.2. Yields

In standard models the yields depend both on the 2DUP and on the interplay between 3DUP and HBB during the TP-AGB phase. This is not the case in the rotating models where the pattern is already well established after the 2DUP since at that time a large fraction of the envelope mass has already been ejected.

In the rotating models, case (B) shows the highest yields (Figure 4) as a result of a deeper 2DUP. The small differences between cases (C) and (D) reflect the small impact of 3DUPs in model (C).

The global effect of rotation is to increase the yields of all nuclides with A $<$ 23. Concerning the abundances of higher mass elements, they are more dependent on both deeper 2DUP and/or mixing processes as illustrated by case (B).

In Figure 4 we have also included the predictions of Meynet & Maeder (2002) for the

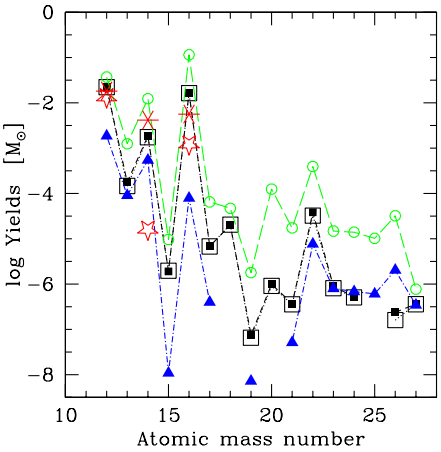

Fig. 4. Yields for the different models : case A (standard, triangles), case B (empty circles), case C (filled squares) and case D (empty squares). Only the elements with positive yields are presented. We also indicate the results of Meynet & Maeder (2002) for their rotating model (asterisks) and their standard model (stars) of a 7 $M_{\odot}$, $Z = 10^{-5}$ star

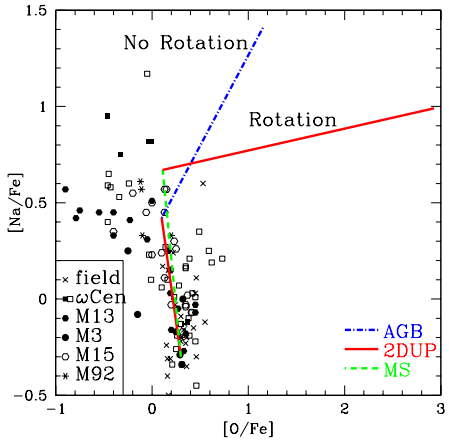

Fig. 5. O-Na anti-correlation in several globular clusters (data from Weiss et al. 2000). We also show the main evolution of the surface abundances for our rotating (case D) and non-rotating models

CNO yields in 7 $M_{\odot}$ stars at $Z = 10^{-5}$ (with and without rotation). Our results agree fairly well with theirs, although some discrepancies can be seen. The ^{14}N yield from the non-rotating model of Meynet & Maeder is lower than ours. This can be easily understood provided that Meynet & Maeder (2002) stopped their models at the end of core He burning. As a consequence, they do not account for the subsequent ^{14}N enhancement that results from hot bottom burning during the TP-AGB phase.

2.3. O-Na anti-correlation in globular clusters

It has been frequently suggested that the O-Na anti-correlation observed in globular cluster stars (i.e. Cottrell & Da Costa 1981) may result from intra-cluster pollution by the winds of massive AGBs. Recently, different studies pointed out the difficulty to reproduce this feature with low metallicity AGB stars without a fine tuning of the mixing parameters (Denissenkov & Herwig 2003, Herwig 2004). The same conclusion was reached by Fenner et al. (2004) in their simulations of globular cluster chemical evolution including the yields of standard AGB model. At present, no models including rotational mixing have been computed to address this issue.

Figure 5 shows the evolution of oxygen and sodium abundances at the surface of our models. In case (A), a slight anti-correlation is produced as a result of 2DUP. But it is afterwards erased by the 3DUP, which raises the [O/Fe]. A correlation is finally obtained between O and Na in contradiction with the observations, as shown by the previously quoted studies.

In cases (B-D), the surface oxygen abundance is slightly decreased by internal diffusion during the main sequence and central He-burning. But the 2DUP reverts this trend and the oxygen abundance raises sharply. The subsequent TP-AGB phase does not modify this abundance even with the weak 3DUP in case (C).

Rotation amplifies the discrepancy between model predictions and observations concerning the [O/Fe]. Therefore rotating massive AGB stars do not likely contribute to the O-Na

anti-correlation in globular clusters during the TP-AGB phase.

3. Conclusion

Models of 7 $M_{\odot}$ star at $Z = 10^{-5}$ have been computed assuming different types of mixing. Our main results for rotating models are that:

- rotation increases the total lifetime and the CO core mass by about 10% compared to standard models;
- the second dredge-up is responsible for the largest modifications of the surface abundance patterns;
- a huge mass loss is experienced during the early-AGB phase;
- their yields are higher and result mostly from the effects of the 2DUP;
- they produce a large amount of primary ^{14}N;
- they are not likely to be responsible for the O-Na anti-correlation seen in globular clusters.

Acknowledgements. TD and CC wish to thank G. Meynet for helpful discussions about rotation. LS is FNRS scientific research worker and AP acknowledges financial support from ESA PRODEX 90069.

References

Alexander D. R., Ferguson J. W., 1994, ApJ, 437, 879
Angulo C. et al., 1999, Nucl. Phys. A, 656, 3
Blöcker T., 1995, A&A, 297, 727
Caughlan G. R., Fowler W. A., 1988, ADNDT, 40, 283
Cottrell P. L., Da Costa G. S., 1981, ApJ, 245, L79
Denissenkov P. A., Herwig F., 2003, ApJ, 590, L99
Fenner Y., et al., 2004, MNRAS, 280
Forestini M., Arnould M., Paulus G., 1991, A&A, 252, 59
Herwig F., 2000, A&A, 360, 952
Herwig F. 2004, ApJ, 605, 425
Iglesias C. A., Rogers F. J., 1996, ApJ, 464,943
Langer N., et al., 1999, A&A, 346, L37
Maeder A., Meynet G., 2001, A&A, 373, 555
Maeder A., Zahn J. P., 1998, A&A, 334, 1000
Meynet G., Maeder, A., 2002, A&A, 390, 561
Palacios A., et al., 2003, A&A, 399, 603
Palacios A., et al., 2005, in preparation
Reimers D., 1975, psae.book, 229
Siess L., Dufour E., Forestini M., 2000, A&A 358, 593
Siess L., Forestini M., Bertout C., 1997, A&A 326, 1001
Weiss A.,Denissenkov P.A., Charbonnel C., 2000, A&A, 356,181
Zahn J. P. 1992, A&A, 265, 115